Urol Res (2007) 35:89–99
DOI 10.1007/s00240-007-0082-8

ORIGINAL PAPER

Successful formation of calcium oxalate crystal deposition in mouse kidney by intraabdominal glyoxylate injection

Atsushi Okada · Shintaro Nomura · Yuji Higashibata · Masahito Hirose · Bing Gao · Mugi Yoshimura · Yasunori Itoh · Takahiro Yasui · Keiichi Tozawa · Kenjiro Kohri

Received: 2 September 2006 / Accepted: 25 January 2007 / Published online: 14 February 2007
© Springer-Verlag 2007

Abstract The establishment of an experimental animal model would be useful to study the mechanism of kidney stone formation. A calcium kidney stone model in rats induced by ethylene glycol has been used for research; however, to investigate the genetic basis affecting kidney stone formation, which will contribute to preventive medicine, the establishment of a kidney stone model in mice is essential. This study indicates the optimum conditions for inducing calcium oxalate stones in normal mouse kidney. Various doses of oxalate precursors, ethylene glycol, glycolate and glyoxylate, were administered either by free drinking or intraabdominal injection for 2 months as a preliminary study. Stone formation was detected with light microscopy, polarized light optical microscopy and electron microscopy. Stone components were detected with X-ray diffraction analysis. The expression of osteopontin (OPN), a major stone-related protein, was detected with immunohistochemical staining, in situ hybridization and quantitative reverse transcriptase polymerase chain reaction. Kidney stones were not detected in ethylene glycol- or glycolate-treated groups even at the highest dose of LD_{50}. Whereas, numerous kidney stones were detected in glyoxylate-treated mice (more than 60 mg/kg) at 3, 6 and 9 days after glyoxylate were administered intraabdominally. However, the number of kidney stones decreased gradually at day 12, and was hardly detected at day 15. The stone component was further analyzed as calcium oxalate monohydrate. A dramatic increase in the expression of OPN was observed by the administration of glyoxylate. We established a mouse kidney stone experimental system in this study. The difficulty of inducing kidney stones suggested that mice have greater intrinsic ability to prevent stone formation with hyperoxaluric stress than rats. The differing response to hyperoxaluric stress between mice and rats possibly contributes to the molecular mechanism of kidney stone formation and will aid preventive medicine in the future.

Keywords Osteopontin · Kidney stone · Model mouse · Calcium oxalate · Glyoxylate

A. Okada (✉) · Y. Higashibata · M. Hirose · B. Gao · M. Yoshimura · Y. Itoh · T. Yasui · K. Tozawa · K. Kohri
Department of Nephro-urology, Nagoya City University Graduate School of Medical Sciences, 1 Kawasumi, Mizuho-cho, Mizuho-ku, Nagoya City, Aichi 467-8601, Japan
e-mail: a-okada@med.nagoya-cu.ac.jp

S. Nomura
Department of Pathology, Osaka University Graduate school of Medicine, 2-2, Yamada-oka, Suita City, Osaka, Japan

Introduction

Investigation of the kidney stone formation process in animals has long been limited to hyperoxaluric rat experimental models by the administration of metabolic intermediates of oxalate, such as ethylene glycol, glycolate or glyoxylate [1–6] (Fig. 1). This model remains controversial as to whether it is an experimental and clinical stone model; however, Yamaguchi et al. [7] and Umekawa et al. [8] reported that a rat model of calcium oxalate stone formation did not show severe renal damage and could be a clinical kidney stone model. Using this model, many gene expressions were related to stone formation, such as osteopontin [2, 9, 10], Tamm-Horsfall protein [11], heparan sulfate/heparan sulfate

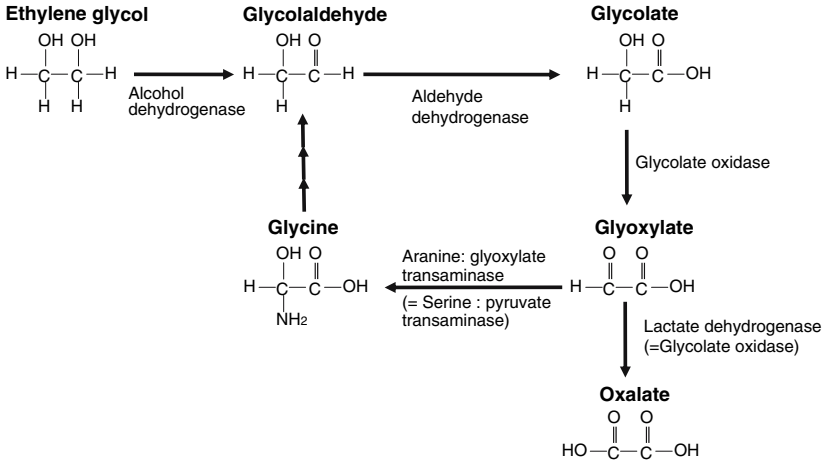

Fig. 1 The major metabolic pathway of ethylene glycol to oxalate (mainly in peroxysome in hepatocytes). The metabolic pathway is used for plant-derived oxalate metabolites in herbivorous animals (Ref. [31])

proteoglycan [12], bikunin [12] or inter-alpha inhibitor-related proteins [13]. In addition, this model is useful to investigate the effect of stone preventive agents such as vitamin E [14, 15], citrate [9, 16] or alloprinol [10].

Our investigations have focused on OPN [1,17], identified as a major organic component of kidney stones in humans and rats [17, 18]. Changes in the expression level of OPN during experimental crystal formation have been extensively studied in rat models. After 4 weeks of ethylene glycol administration to rats, a dramatic increase in the expression of OPN protein and mRNA [17–19] was found in the epithelial cells of distal tubules and the resulting kidney stones also contained OPN.

Recently, genome-wide expression research such as the microarray technique has been introduced to identify the genes responsible for objective phenomena or disease. As for kidney stones, a rat experimental model was used for microarray analysis and several genes involved in the inflammatory reaction or cell adaptation, including OPN, were detected [6]. To investigate the accurate function of the objective gene, a transgenic mouse study, including a knockout mouse, is very useful. Several studies indicated the function of stone-related protein using knockout mice. Wesson et al. [20] reported that the administration of 1% ethylene glycol in free drinking could induce stone formation in OPN knockout mice kidney, but not in wild-type mice. Mo et al. [21] indicated that Tamm-Horsfall protein (THP) knockout mice generated calcium oxalate (CaOx) stones in the kidney by introducing 1% ethylene glycol and vitamin D3. The establishment of a system to induce kidney stones in normal mice is very important since the system can verify whether the process of kidney stone formation in these knockout mice is physiological. The system will contribute to clinical research, which will control genetic effects on kidney stone formation in the near future.

This study was performed to establish a method and conditions for inducing kidney stones in normal mouse kidney. The successful effect of glyoxylate in the formation of kidney stones is described. In addition, the relationship between stone formation and OPN expression is discussed.

Materials and methods

Preliminary experiment for inducing kidney stones in normal mice kidney by administration of oxalate precursors

All animal studies followed the recommendations of the NIH Guide for the Care and Use of Laboratory Animals.

To induce CaOx kidney stones in mouse kidney, three types of oxalate precursor, ethylene glycol, glycolate and glyoxylate, were introduced using two methods into previously reported rat experimental nephrolithiasis models [1–6]. Briefly, all prepared oxalate precursors were kept at 4°C until administration. In free drinking, mice had access to a bottle of tap water. Intraabdominal injection was performed according to the weight of each mouse with a clean 27-gauge needle every day. All animals had free access to standard chow and water. The amount of administered oxalate precursors is indicated in Table 1.

Detection of kidney stone formation

Renal specimens were fixed in 4% paraformaldehyde, and embedded in paraffin. Four-micrometer-thick cross-sections were stained with the previous described

Table 1 Preliminary data of mouse kidney crystal formation induced by three types of oxalate precursor

Administered oxalate precursor		Length of administration				
		3 days	7 days	14 days	28 days	56 days
Ethylene glycol						
FD						
1%	(0.16 mol/l)	0 [0/12]	0 [0/5]	0 [0/13]	0 [0/31]	0 [0/4]
5%	(0.81 mol/l)	0 [0/5]	0 [0/12]	0 [0/10]	0 [0/10]	0 [0/2]
10%	(1.61 mol/l)	0 [0/3]	0 [0/6]	Not alive	Not alive	Not alive
IAI						
100 mg/kg	(1.61 mmol/kg)	0 [0/6]	0 [0/7]	0 [0/8]	0 [0/10]	0 [0/3]
500 mg/kg	(8.06 mmol/kg)	0 [0/3]	0 [0/6]	0 [0/6]	0 [0/6]	0[0/8]
1,000 mg/kg	(16.1 mmol/kg)	0 [0/4]	0 [0/6]	0 [0/4]	0 [0/6]	Not alive
5,000 mg/kg	(80.6 mmol/kg)	0 [0/5]	0 [0/3]	Not alive	Not alive	Not alive
Glycolate						
FD						
1%	(0.13 mol/l)	0 [0/3]	0 [0/3]	0 [0/7]	0 [0/6]	0 [0/3]
5%	(0.66 mol/l)	0 [0/3]	0 [0/3]	0 [0/7]	0 [0/3]	Not alive
10%	(1.31 mol/l)	0 [0/4]	Not alive	Not alive	Not alive	Not alive
IAI						
60 mg/kg	(0.78 mmol/kg)	0 [0/3]	0 [0/3]	0 [0/3]	0 [0/7]	0 [0/3]
100 mg/kg	(1.31 mmol/kg)	0 [0/3]	0 [0/3]	0 [0/3]	0 [0/3]	0 [0/3]
120 mg/kg	(1.31 mmol/kg)	0 [0/3]	0 [0/3]	0 [0/3]	Not alive	Not alive
Glyoxylate						
FD						
1%	(0.14 mol/l)	0 [0/3]	0 [0/5]	0 [0/5]	0 [0/5]	0 [0/5]
5%	(0.68 mol/l)	0 [0/3]	0 [0/5]	0 [0/5]	0 [0/5]	0 [0/5]
10%	(1.35 mol/l)	0 [0/5]	0 [0/3]	Not alive	Not alive	Not alive
IAI						
50 mg/kg	(0.68 mmol/kg)	0 [0/5]	0 [0/6]	0 [0/6]	0 [0/6]	0 [0/6]
60 mg/kg	(0.81 mmol/kg)	0.20 [1/5]	0.40 [2/5]	0 [0/8]	0 [0/6]	0 [0/6]
80 mg/kg	(1.08 mmol/kg)	0.40 [2/5]	1.00 [5/5]	0 [0/8]	0 [0/5]	Not alive
100 mg/kg	(1.35 mmol/kg)	0.40 [2/5]	1.00 [5/5]	0 [0/12]	0 [0/3]	Not alive
150 mg/kg	(2.03 mmol/kg)	1.00 [5/5]	Not alive	Not alive	Not alive	Not alive

The value of oxalate precursors indicates the daily injection dose

Square brackets indicate stone formation rates (number of mice showing kidney stone formation/total number of mice administered each oxalate precursor)

FD freedrink, *IAI* intraabdominal injection

Pizzolato staining method [22] to detect oxalate-containing crystals. Briefly, dewaxed paraffin sections and bring to distilled water as usual. Mix 30% hydrogen peroxide and 5% silver nitrate, 1 ml each, and pour onto the slide with tissue sections (pH of this mixture is 6.0). Expose slide to light from a 60-W incandescent lamp at a distance of 15 cm (6 in.) for 15–30 min. Numerous gas bubbles develop and it is necessary to pour off the mixture and add a fresh solution. Wash the slide thoroughly with distilled water and counterstain with safranin, and then dehydrate in the usual manner.

To identify generated Pizzolato positive-stained substances such as stones, polarized light optical microphotography (BX51–33P-O, Olympus, Tokyo, Japan) was used to observe the same sections.

Confirmation study for kidney stone formation by glyoxylate administration

Forty-two C57BL/6 male mice (8 weeks old) were administered 80 mg/kg glyoxylate by daily intraabdominal injection. The adapted administration method used in this study was optimized by preliminary experiments (Table 1).

The experiment was conducted for the following 15 days. At designated time points (days 0, 3, 6, 9, 12 and 15), the kidneys were extracted to examine CaOx stone formation, RNA preparation and immunohistochemical study ($n = 7$ at each time point).

Five mice were placed in metabolic cages the day before each treatment day and 24 h urine samples were collected. Urinary volume, pH, calcium, phosphorus, magnesium, oxalate and citrate were determined at each time point (SRL, Inc., Tokyo, Japan). The ion-activity product of the calcium oxalate [AP(CaOx)] index was calculated according to the formula for rat urine [32].

Kidney stone formation was detected by Pizzolato staining and polarized light optical microphotography as described above. For the quantification of stone formation, Pizzolato positive-staining regions were measured and expressed as percentages of the total tissue area of cross-sections of the kidney with soft NIH image 1.61 (Scion Inc., USA).

Inorganic components of stones were determined with X-ray diffraction (XRD). Ten calcified kidneys (sixth and ninth day) identified in preliminary study were frozen, crushed and placed in a sample holder, then qualitative and quantitative analyses were performed with XRD-6100 (Shimazu, Tokyo, Japan).

Quantitative RT-PCR

Total RNA was isolated from frozen sections of mouse kidney samples with ISOGEN (Nippon Gene Co., Ltd., Toyama, Japan) according to the manufacturer's instructions. TaqMan® Gene Expression Assay (Applied Biosystems, Foster City, CA), 20× assay mix of primers and TaqMan® MG probes (FAM™ dye-labeled) for OPN mRNA (Mm00436767_m1, Applied Biosystems) were used for quantitative RT-PCR [23] using the ABI PRISM®7700 Sequence Detection System (Applied Biosystems). This assay was designed to span exon–exon junctions so as not to detect genomic DNA, and these primers and probe sequences were searched against the Celera database to confirm specificity. Validation experiments were performed to test the efficiency of the target amplification and the efficiency of the reference amplification. OPN mRNA amplification was compared with the amplification of standard oligo-DNA fragments prepared previously by RT-PCR using the same primer sets and their concentration and absolute copy numbers were determined with a standard curve and corrected with the amount of total RNA. One-Step RT-PCR reactions using TaqMan® One-Step RT-PCR Master Mix Reagent Kit (4309169, Applied Biosystems) were started with an initial reverse transcription step at 48°C for 30 min. After denaturing at 95°C for 10 min, PCR was started at 95°C for 15 s and completed at 60°C for 1 min. The PCR reaction was repeated 40 times. The reaction component consisted of 25 µl of 2× Master Mix, 1.25 µl of 40× MultiScribe and RNase Inhibitor Mix, 2.5 µl of OPN expression quantitative primer and 400 ng/ml total RNA sample.

Immunohistochemical staining

Immunohistochemical staining was carried out on sections treated with microwaves for 15 min and blocked with 0.5% H_2O_2 in methanol for 30 min, followed by washing in 0.01 M phosphate-buffered saline (PBS) and further treated with skimmed milk in PBS for 1 h at room temperature. These slides were then incubated with polyclonal anti-mouse OPN rabbit IgG (IBL Co., Ltd., Gunma, Japan). The reacted antibody was detected using a VECTASTAIN® Elite ABC kit for rabbit IgG (Vector Laboratories, Inc., Burlingame, CA, USA) according to the manufacturer's instructions.

In situ hybridization

Digoxigenin (DIG)-uridine triphosphate (UTP)-labeled single-strand sense and antisense mouse OPN RNA probes [17] were prepared for hybridization using a DIG RNA labeling kit (Rosh Diagnostic, IN, USA) according to the manufacturer's instructions.

Kidney tissue samples for in situ hybridization were placed in 4% paraformaldehyde in 0.1 M phosphate buffer (pH 7.0), dehydrated in ethanol and embedded in paraffin under RNase-free conditions: serial sections, 5 µm thickness, were cut. Details of the in situ hybridization technique have been described previously [24]. A hybridization solution containing approximately 0.5 µg/ml of cRNA probes was placed on each section, and hybridization was performed at 50°C for 16 h. Hybridized DIG-cRNA probes were detected by alkaline phosphatase conjugated with anti-DIG antibody (Fab fragment).

Transmission electron microscopy

For observation of the super microstructure of kidney stone formation, another six mice were administered 80 mg/kg of glyoxylate for 3, 6 and 9 days in addition to the 42 mice. At the each time point, two mice were sacrificed and kidneys were extracted. The kidneys were perfused with phosphate-buffered saline (PBS) and 2.5% of glutaraldehyde through the left ventricle of the heart. The kidneys were tied and excised. Small tissue blocks from the cortex and medulla were fixed with 2% of OsO4 for 2 h, and then dehydrated in ethanol and embedded in epoxy resin. Semi-ultrathin sections (0.2–0.5 µm) were made and stained with uranyl acetate and lead citrate, and examined with a JEM-1011 (JEOL Ltd., Tokyo, Japan).

Statistical analysis

The number of mice studied per group is indicated for each experiment and the means ± SE are shown. For estimation of the change of kidney stone formation and elimination, Spearman's rank correlation test was used. Statistical analysis of OPN mRNA expression by quantitative RT-PCR was performed using Student's *t*-test. A probability of 0.05 was taken as statistically significant.

Results

Mouse kidney stone formation in preliminary administration of oxalate precursors

The results of administering three types of oxalate precursor are shown in Table 1. Ethylene glycol and glycolate could not induce kidney stones at any concentration using free drinking water or intraperitoneal injection for 2 months; however, intraperitoneal injection of glyoxylate, higher than 60 mg/kg, could induce kidney stone formation at day 3 after administration. These stones showed strong birefringence by polarized light optical microphotography (Fig. 2). The stones were generated mainly in renal tubules located at the border between the renal cortex and medulla.

Confirmation of kidney stone formation and elimination

At 3 days after administration, kidney stone formation was confirmed as a preliminary study. The number of kidney stones increased and peaked at day 6; however, they decreased thereafter, and were hardly detectable on day 15 (Fig. 3a), even by polarized light optical microphotography (data not shown). By quantitative analysis of stone formation (Fig. 3b), the increase of kidney stones from 0 to 6 days and decrease from 6 to 15 days changed significantly (0–6 days: $r = 0.084$, $P < 0.0001$, 6–15 days: $r = -0.053$, $P < 0.0001$; Spearman's rank correlation test).

X-ray diffraction identified that the major component of kidney calcification was calcium oxalate monohydrate (COM) (Fig. 3C). XRD patterns of kidney tissue were identical and showed multiple diffraction peaks characteristic of COM and no peaks characteristic of calcium oxalate dihydrate or others.

Urinary biochemistry

Urinary parameters, including the urinary creatinine index and 24-h urine values at each time point, are shown in Table 2. Urinary oxalate levels were remained similar throughout the experimental course. However, the 24-h oxalate value on day 15 was higher than that on day 0 ($P < 0.05$). Urinary calcium levels were higher on day 12 ($P < 0.05$), and also higher in relation to the creatinine index ($P < 0.01$). 24-h calcium value on day 15 was higher than that on day 0 ($P < 0.05$). Urinary levels and 24-h values of phosphorus remained similar during the experimental course. Urinary levels and 24-h values of citrate and magnesium were slightly lower on day 6 but remained similar throughout the experimental course. Urinary creatinine levels remained similar throughout the experiment. Urinary pH values were significantly lower on day 6 ($P < 0.05$). AP(CaOx) values were significantly higher on day 12 ($P < 0.01$).

Expression of OPN during stone formation

Changes in the spatial expression of OPN during stone formation were examined by quantitative RT-PCR,

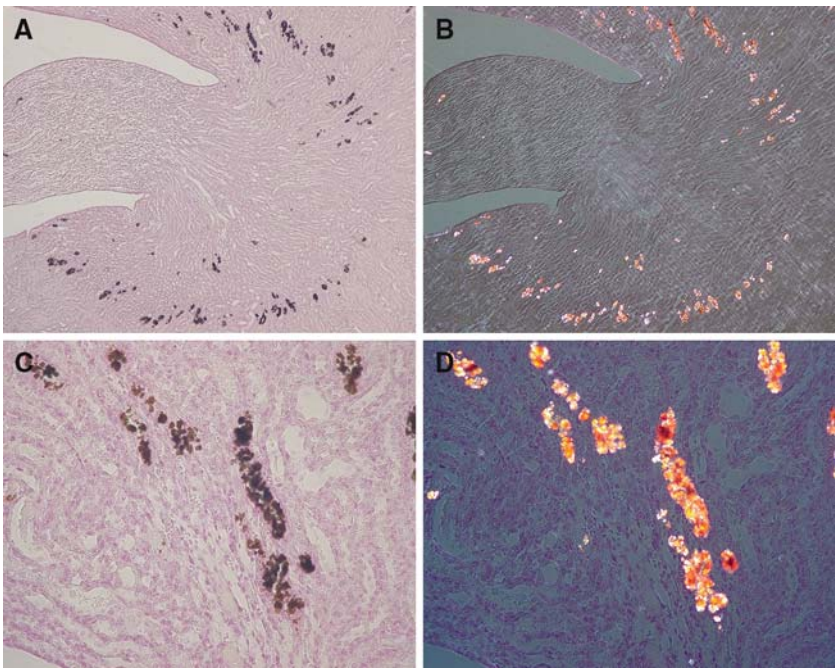

Fig. 2 Kidney crystallization generated by glyoxylate administration. **a**, **c** Pizzolato staining showed brown-stained calcium oxalate crystal retention in the distal tubules between the renal cortex and medulla. **b**, **d** Polarized light optical microphotography in the same field as (**a**) and (**c**). Strong birefringence was detected coinciding with Pizzolato-stained crystals (magnification **a**, **b** ×100, **c**, **d** ×400)

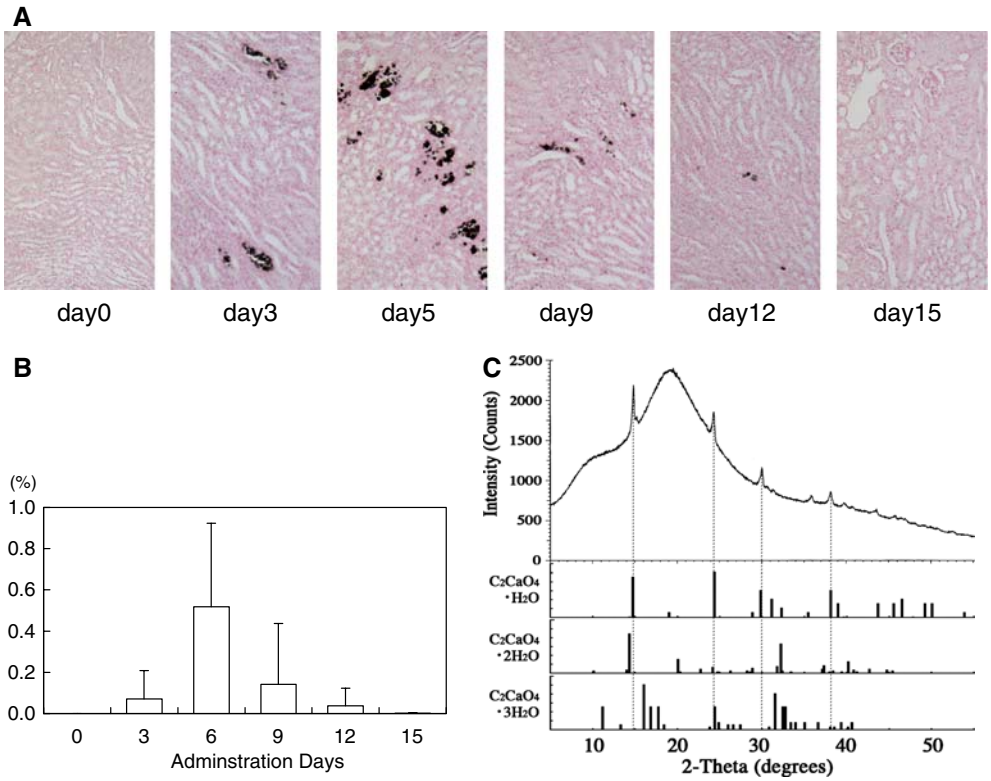

Fig. 3 Changes in the amount of kidney crystals generated by administration of glyoxylate formation through the experimental course. **a** Pizzolato-stained kidney sections administered with glyoxylate at each time point of the experimental course (magnification ×200). The amount of crystallization in each kidney section was quantified by calculating the ratio of Pizzolato-stained regions to the kidney section using NIH image 1.61. **b** Changes in the amount of crystals during the experimental course (data are presented as the mean ± SE.) **c** Crystal components in mice kidneys were isolated as calcium oxalate monohydrate ($C_2CaO_4 \bullet H_2O$) crystals with X-ray diffraction (*XRD*) analysis. XRD patterns have multiple diffraction peaks characteristic of the registered patterns of calcium oxalate monohydrate in the XRD peak pattern database (lower graph) and no peaks characteristic of calcium oxalate dihydrate ($C_2CaO_4 \bullet 2H_2O$) or calcium oxalate trihydrate ($C_2CaO_4 \bullet 3H_2O$)

in situ hybridization and immunohistochemistry (Fig. 4). By quantitative RT-PCR, the expression at day 3 increased significantly (about 22 times as high as day 0, $P < 0.0001$), decreased subsequently and reached a certain level at day 15 (about five times as high as day 0, $P = 0.0375$) (Fig. 4a). By in situ hybridization, OPN mRNA was detected in renal tubules (Fig. 4b). Immunohistochemical analysis demonstrated the presence of OPN in the tubules and stones (Fig. 4c). The results indicated a transitory increase and focal expression in specific distal tubules at day 3, followed by a gradual decrease and extension to the whole kidney from day 6 to 15 (Fig. 4b, c), which seemed to be the same tendency as quantitative RT-PCR

Transmission electron microscopy

In semi-ultrasections of renal specimens from day 6, there were many rod-shaped crystals with high electrodensity retained in the proximal tubular lumens. These crystals aggregated and formed rosettes including low-density colloid materials (Fig. 5a).

In the section from day 9, fragmented small crystals existed in the cytoplasm of multinucleate giant cells, which possessed numerous mitochondria, vacuoles and very high dense vesicles considered as lysosomes in the cytoplasm (Fig. 5b).

Discussion

Mice are frequently used in medical experiments. However, it was long believed that they were not suitable for urolithiasis experiments because kidney stones in mice could not be induced with hyperoxaluric stress as in rat experimental models. In this study, we developed an experimental system for inducing kidney stones in normal mice. An intraabdominal injection of glyoxylate was effective to induce experimental kidney

Table 2 Values on urinary biochemistry of glyoxylate-treated mice

	0 day	3 day	6 day	9 day	12 day	15 day
Oxalate (mg/l)	17.75 ± 1.69	18.43 ± 8.01	13.53 ± 4.01	15.43 ± 4.53	17.12 ± 6.33	22.28 ± 13.08
Calcium (mg/dl)	4.41 ± 1.09	6.18 ± 3.35	2.71 ± 0.78	8.30 ± 4.56	12.99 ± 12.86*	9.16 ± 4.01
Phosphorus (mg/dl)	117.40 ± 62.74	96.20 ± 21.90	121.10 ± 50.20	145.80 ± 62.49	111.64 ± 77.56	145.10 ± 91.28
Citrate (mg/dl)	815.94 ± 712.69	642.24 ± 732.18	37.89 ± 6.40*	691.85 ± 929.67	400.89 ± 715.83	1503.62 ± 1666.45
Magnesium (mg/dl)	40.64 ± 13.46	29.12 ± 21.26	15.56 ± 9.98	37.33 ± 6.90	28.62 ± 22.43	49.86 ± 30.18
Creatinine (mg/dl)	25.51 ± 4.26	19.00 ± 6.47	15.67 ± 1.64	19.01 ± 4.16	15.28 ± 4.64	23.57 ± 15.76
Indexed to creatinine						
Oxalate (mmol/g) creatinine	0.80 ± 0.19	1.11 ± 0.53	0.96 ± 0.29	0.90 ± 0.17	1.37 ± 0.81	1.29 ± 0.72
Calcium (mmol/g) creatinine	4.44 ± 1.50	8.04 ± 3.60	4.27 ± 0.88	11.42 ± 6.86	19.07 ± 14.27**	11.74 ± 4.14
Phosphorus (mmol/g) creatinine	142.00 ± 56.95	169.92 ± 42.65	250.50 ± 110.73	271.39 ± 181.58	222.20 ± 104.30	214.24 ± 51.75
Citrate (mmol/g) creatinine	16.00 ± 13.69	17.80 ± 23.47	1.28 ± 0.30	18.57 ± 21.94	10.86 ± 18.17	23.85 ± 19.39
Magnesium (mmol/g) creatinine	64.38 ± 12.07	59.78 ± 32.37	39.28 ± 22.87	82.14 ± 13.21	70.08 ± 44.86	89.26 ± 11.80
24-h urine biochemistry						
Volume (ml/day)	0.96 ± 0.41	1.25 ± 0.49	1.23 ± 0.70	0.75 ± 0.13	0.73 ± 0.35	1.35 ± 0.86
Oxalate (μmol/24 h)	1.85 ± 0.63	2.26 ± 0.62	1.72 ± 0.81	1.25 ± 0.26	1.22 ± 0.26	2.61 ± 0.71*
Calcium (μmol/24 h)	1.06 ± 0.53	1.81 ± 0.90	0.85 ± 0.60	1.59 ± 1.07	2.05 ± 1.34	2.45 ± 0.48*
Phosphorus (μmol/24 h)	42.47 ± 35.22	36.79 ± 10.48	49.82 ± 30.03	34.82 ± 14.32	21.98 ± 11.04	46.99 ± 16.49
Citrate (μmol/24 h)	347.49 ± 341.41	312.01 ± 420.21	19.05 ± 12.39	229.77 ± 328.32	78.42 ± 129.93	464.56 ± 379.37
Magnesium (μmol/24 h)	17.40 ± 12.05	13.82 ± 7.74	9.30 ± 9.34	11.69 ± 3.87	8.54 ± 5.57	20.12 ± 7.55
Creatinine (μmol/24 h)	2.28 ± 1.30	1.95 ± 0.48	1.73 ± 1.03	1.26 ± 0.36	0.96 ± 0.48	1.98 ± 0.66
pH	7.25 ± 0.65	6.38 ± 0.48	6.20 ± 0.44*	6.38 ± 0.48	7.00 ± 0.58	6.63 ± 0.25
AP (CaOx)	1.40 ± 1.17	2.53 ± 1.92	1.95 ± 0.83	2.34 ± 1.70	4.68 ± 2.35**	2.10 ± 0.77

*$P < 0.05$, **$P < 0.01$ (P values indicate the statistical significance of the changes in the urine parameters measured at 0 day and at each time points)

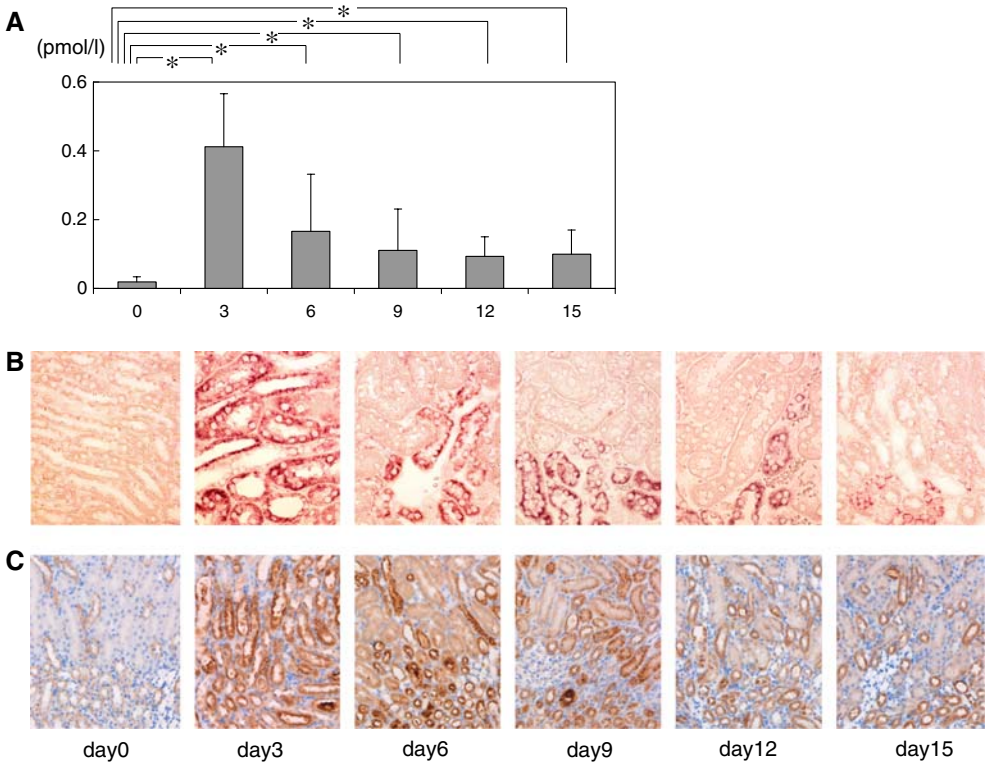

Fig. 4 Changes in the expression of OPN mRNA and protein in mice kidneys during the experimental course by the administration of glyoxylate. **a** Quantification of OPN mRNA expression of the kidney by quantitative reverse transcription polymerase chain reaction (RT-PCR) (*$P < 0.01$ compared with day 0. Data are presented as the mean ± SE.). **b** In situ hybridization for OPN mRNA and immunohistochemical staining for OPN protein (**c**) (magnification ×200). Both experiments showed that OPN expression in the early phase occurred focally in particular distal tubular cells and spread to whole kidney sections throughout the time course. In crystal-formed sections of immunohistochemically stained kidney, dark-stained OPN-containing crystals in the distal tubules were detected

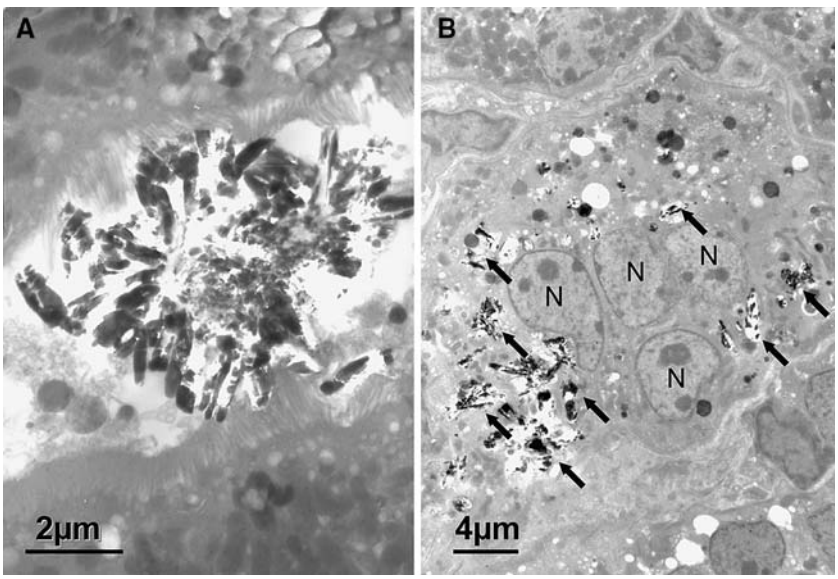

Fig. 5 **a** Electron micrograph of a detail of intratubular stone formation. In the cavity surrounded by proximal renal tubular cells with a brush border, high-density crystals are retained, forming rosettes and involving some colloid materials. **b** Electron micrograph of details of interstitial multinucleate giant cells, showing several crystals (*arrows*). Several nuclei (*N*) can be recognized. Tissues were obtained from glyoxylate-treated mice for 6 days (magnification ×8,000, 500 nm semi-ultra cut) and 9 days (magnification ×2,500, 500 nm semi-ultra cut), respectively

stones in a mouse model. This result was induced from preliminary experimental data, and some problems remained to be solved in the accurate amount of oxalate precursor the animal is actually being given and the amount of oxalate excreted in urine. These points need further verification in the future.

The optimum condition for kidney stone formation in mice is completely different from the rat experimental

system. Rats have been used for decades as a kidney stone model induced by the administration of oxalate precursors indicated in Fig. 1. Among many methods, free drinking of 1% ethylene glycol is the easiest method [1, 2, 6] with advantages of the method being that animals did not need to be handled on a daily basis. However, the critical concentration of ethylene glycol or glycolate could not induce kidney stone formation in mouse kidney, regardless of adequate values matched to glyoxylate load. There are species differences between mice and rats, although they are both rodents, related to calcium oxalate experimental kidney stone formation.

The reason for this species difference, especially the efficacy of glyoxylate and ethylene glycol, is unknown. Among the possibilities, metabolism in the liver or the toxicity of each oxalate precursor in the kidney should be investigated. There is no report referring to species differences in the facility of kidney stone formation between rats and mice. Meanwhile, in toxicology lesions, species differences of organ reactions to particular toxic agents have often been investigated. Shimada et al. [25] reported that limonene, a kind of terpene found in orange peel and other plants, caused renal toxicity in male rats, but not in female rats and other species of animals including mice, rabbits, guinea pigs, and dogs.

Yoshihara et al. [26] reported that glyoxylate tends to be metabolized to oxalate in male rats and to glycine in females. The difference is the result of the enzymatic balance of glycolate oxidase and serine pyruvate transaminase in rat liver affected by sex hormones. Our results might involve species differences of oxalate metabolism in the liver, which is an important issue to be investigated hereafter. However, urinary biochemistry did not show any significant increase in urinary oxalate excretion during the stone formation period, therefore the keys for stone formation in the mouse kidney seemed to involve other factors.

Poldelski et al. [27] reported the cytotoxicity of oxalate precursors and investigated the influence of cell damage by ethylene glycol, glycol aldehyde and glyoxylate, concluding that glyoxylate has stronger cytotoxicity than other precursors. Kidney stones could be induced in mice under very limited conditions. The difference in the result of kidney crystallization between glyoxylate and ethylene glycol (and glycolate) may depend on the different cytotoxicity of these substances. During the stone formation period until day 6, urinary pH decreased to a significantly lower level (pH = 6.2, $P = 0.0050$), and urinary excretion of citrate and magnesium demonstrated lower levels (not significant). Stone formation in mouse kidney may depend on the combination of this acidified condition of urine and cytotoxicity caused by glyoxylate (pH = 2).

Changes in the expression level of OPN during kidney stone formation in mice showed a temporary increase at day 3 after the administration of glyoxylate. The expression pattern was different from rat experimental models that maintained a considerably high level during the period of administration [17]. The difference in osteopontin expression between rats and mice may relate to the facility of kidney stone formation in rats. The role of OPN in kidney stone formation is still controversial. However, the pattern of increased kidney stone formation delaying the peak of OPN expression suggests OPN as one of promoters of experimental kidney stone formation in mice. A mouse model of kidney stone formation has now been established and consecutive OPN knockout studies using the glyoxylate-induced method will lead to elucidation of the role of OPN in kidney stone formation.

We found that kidney stones in mice gradually decreased 6 days after administration, and were significantly and completely eliminated in spite of the uninterrupted administration of glyoxylate. These findings suggested that mouse kidneys can eliminate calcium oxalate deposition, and have developed the ability to prevent more stone formation during hyperoxaluric stress. Several reports have referred to the possibility of stone elimination. De Water et al. [28] reported that the amount of kidney-associated oxalate diminished with time, which may have been caused by the removal of interstitial crystals through the endocytosis of multinucleate giant cells from findings of immunohistochemistry and electron microscopy. In our study, we also detected interstitial multinucleate giant cells with endocytosis of small crystals, and such observations also confirm the results of a previous study on hyperoxaluric rats and chronic oxalosis in humans [29]. It has been reported that CaOx crystals can activate the ability of macrophages to resorb bone [30]. Urinary CaOx crystals have a stone matrix of organic substances, including OPN. If the matrix of these crystals can be dissolved by the release of proteolytic enzymes, CaOx crystals will be fragmented into composing nanometer-sized particles [30]. In our study, urinary calcium and oxalate levels increased on day 12 or day 15 with increase of AP(CaOx), which did not correlate with stone number but might imply the consequence of treating CaOx crystals by interstitial multinucleate giant cells. Our results may support their hypothesis of the ability to remove kidney stones.

Considering the difficulty of inducing mouse kidney crystals, mice may have strong preventive ability in kidney crystal formation caused by hyperoxaluria and

to eliminate crystals with some renoprotective factors. The mouse kidney could have a protective mechanism, which could become effective after several days of exposure to a toxin. This mechanism could prevent the formation of new crystals and foster the removal of already formed crystals.

Taken together, we produced a foothold for the investigation of mice kidney stone formation and elimination by establishing a mouse kidney stone model. This experimental kidney stone in hyperoxaluric mice is calcium oxalate nephrocalcinosis, not true stones; however, we believe that this model will provide new knowledge about how to create frequently occurring calcium oxalate stones. This model is also useful for the in vivo study of specific gene functions by using transgenic or knockout technology. Furthermore, stone elimination may be an important key to elucidate possible methods to prevent kidney stones from normal kidneys.

Acknowledgments We would like to thank Ms. A. Makie, Ms. N. Kasuga, Ms. A. Hayashi and Ms. Y. Kobayashi for their expert management of mice and secretarial assistance. This work was supported in part by Grants-in-Aid from the Ministry of Education, Culture, Science and Technology (No. 12307034, No. 13770889, No. 16790922) and the Aichi Kidney Foundation, Japan.

References

1. Khan SR (1995) Experimental calcium oxalate nephrolithiasis and the formation of human urinary stones. Scanning Microsc 9:89
2. Khan SR, Johnson JM, Peck AB, Cornelius JG, Glenton PA (2002) Expression of osteopontin in rat kidneys: induction during ethylene glycol induced calcium oxalate nephrolithiasis. J Urol 168:1173–1181
3. Harris KS, Richardson KE (1980) Glycolate in the diet and its conversion to urinary oxalate in the rat. Invest Urol 18:106–109
4. Kohri K, Nomura S, Kitamura Y, Nagata T, Yoshioka K, Iguchi M, Yamate T, Umekawa T, Suzuki Y, Sinohara H (1993) Structure and expression of the mRNA encoding urinary stone protein (osteopontin). J Biol Chem 268:15180–15184
5. Harris KS, Richardson KE (1980) Glycolate in the diet and its conversion to urinary oxalate in the rat. Invest Urol 18:106–109
6. Katsuma S, Shiojima S, Hirasawa A, Takagaki K, Kaminishi Y, Koba M, Hagidai Y, Murai M, Ohgi T, Yano J, Tsujimoto G (2002) Global analysis of differentially expressed genes during progression of calcium oxalate nephrolithiasis. Biochem Biophys Res Commun 23:544–552
7. Yamaguchi S, Wiessner JH, Hasegawa AT, Hung LY, Mandel GS, Mandel NS (2005) Study of a rat model for calcium oxalate crystal formation without severe renal damage in selected conditions. Int J Urol 12:290–298
8. Umekawa T, Yamate T, Amasaki N, Kohri K, Kurita T (1995) Osteopontin mRNA in the kidney on an experimental rat model of renal stone formation without renal failure. Urol Int 55:6–10
9. Yasui T, Sato M, Fujita K, Tozawa K, Nomura S, Kohri K (2001) Effects of citrate on renal stone formation and osteopontin expression in a rat urolithiasis model. Urol Res 29:50–56
10. Yasui T, Sato M, Fujita K, Ito Y, Nomura S, Kohri K (2001) Effects of allopurinol on renal stone formation and osteopontin expression in a rat urolithiasis model. Nephron 87:170–176
11. Marengo SR, Chen DH, Kaung HL, Resnick MI, Yang L (2002) Decreased renal expression of the putative calcium oxalate inhibitor Tamm-Horsfall protein in the ethylene glycol rat model of calcium oxalate urolithiasis. J Urol 167:2192–2197
12. Eguchi Y, Inoue M, Iida S, Matsuoka K, Noda S (2002) Heparan sulfate (HS)/heparan sulfate proteoglycan (HSPG) and bikunin are up-regulated during calcium oxalate nephrolithiasis in rat kidney. Kurume Med J 49:99–107
13. Moriyama MT, Glenton PA, Khan SR (2001) Expression of inter-alpha inhibitor related proteins in kidneys and urine of hyperoxaluric rats. J Urol 165:1687–1692
14. Sakly R, Chaouch A, el Hani A, Najjar MF (2003) Effects of intraperitoneally administered vitamin E and selenium on calcium oxalate renal stone formation: experimental study in rat. Ann Urol (Paris) 37:47–50
15. Thamilselvan S, Menon M (2005) Vitamin E therapy prevents hyperoxaluria-induced calcium oxalate crystal deposition in the kidney by improving renal tissue antioxidant status. BJU Int 96:117–126
16. Ogawa Y, Tanaka T, Yamaguchi K, Morozumi M, Kitagawa R (1987) Effects of sodium citrate, potassium citrate, and citric acid in preventing experimental calcium oxalate urolithiasis in rats. Hinyokika Kiyo 33:1772–1777
17. Umekawa T, Kohri K, Kurita T, Hirota S, Nomura S, Kitamura Y (1995) Expression of osteopontin messenger RNA in the rat kidney on experimental model of renal stone. Biochem Mol Biol Int 35:223
18. Kohri K, Suzuki Y, Yoshida K, Yamamoto K, Amasaki N, Yamate T (1992) Molecular cloning and sequencing of cDNA encoding urinary stone protein, which is identical to osteopontin. Biochem Biophys Res Commun 184:859
19. Yagisawa T, Chandhoke PS, Fan J, Lucia S (1998) Renal osteopontin expression in experimental urolithiasis. J Endourol 12:171
20. Wesson JA, Johnson RJ, Mazzali M, Beshensky AM, Stietz S, Giachelli C (2003) Osteopontin is a critical inhibitor of calcium oxalate crystal formation and retention in renal tubules. J Am Soc Nephrol 14:139
21. Mo L, Huang HY, Zhu XH, Shapiro E, Hasty DL, Wu XR (2004) Tamm-Horsfall protein is a critical renal defense factor protecting against calcium oxalate crystal formation. Kidney Int 66:1159–1166
22. Pizzolato P (1964) Histochemical recognition of calcium oxalate. J Histochem Cytochem 12:333
23. Gibson UEM, Heid CA, Willams PMA (1996) Novel method for real-time quantitative RT-PCR. Genome Res 6:995
24. Nomura S, Willis AJ, Edward DR, Heath JK, Hogan BLH (1988) Developmental expression of 2ar (osteopontin) and SPARC (osteonectin) RNA as revealed by in situ hybridization. J Cell Biol 106:441
25. Shimada T, Shindo M, Miyazawa M (2000) Species differences in metabolism of (+)- and (−)-limonenes and their metabolites, carneols and carvones, by cytochrome P450 enzymes in liver microsomes of mice, rats, guinea pigs, rabbits, dogs, monkeys, and humans. Drug Metab Phrmacokin 17:507–515
26. Yoshihara H, Yamaguchi S, Yachiku S (1999) Effect of sex hormones on oxalate-synthesizing enzymes in male and female rat livers. J Urol 161:668–673

27. Poldelski V, Johnson A, Wright S, Rosa VD, Zager RA (2001) Ethylene glycol-mediated tubular injury: identification of critical metabolites and injury pathways. Am J Kidney Dis 38:339–348
28. de Water R, Noordermeer C, Houtsmuller AB, Nigg AL, Stijnen T, Schroder FH, Kok DJ (2000) Role of macrophages in nephrolithiasis in rats: an analysis of the renal interstitium. Am J Kidney Dis 36:615–625
29. de Water R, Noordermeer C, van der Kwast TH, Nizze H, Boeve ER, Kok DJ, Schroder FH (1999) Calcium oxalate nephrolithiasis: effect of renal crystal deposition on the cellular composition of the renal interstitium. Am J Kidney Dis 33:761–771
30. de Bruijn WC, de Water R, van Run PR, Boeve ER, Kok DJ, Cao LC, Romijn HC, Verkoelen CF, Schroder FH (1997) Ultrastructural osteopontin localization in papillary stones induced in rats. Eur Urol 32:360–367
31. Poldelski V, Johnson A, Wright S, Rosa VD, Zager RA (2001) Ethylene glycol-mediated tubular injury: identification of critical metabolites and injury pathways. Am J Kidney Dis 38:339–348
32. Tiselius HG, Ferraz RR, Heilberg IP (2003) An approximate estimate of the ion-activity product of calcium oxalate in rat urine. Urol Res 31:410–413